■ BONE BIOLOGY

Development of a rodent high-energy blast injury model for investigating conditions associated with traumatic amputations

Z. Kazezian,
X. Yu,
M. Ramette,
W. Macdonald,
A. M. J. Bull

From Centre for Blast Injury Studies, Imperial College London, London, UK

Aims

In recent conflicts, most injuries to the limbs are due to blasts resulting in a large number of lower limb amputations. These lead to heterotopic ossification (HO), phantom limb pain (PLP), and functional deficit. The mechanism of blast loading produces a combined fracture and amputation. Therefore, to study these conditions, in vivo models that replicate this combined effect are required. The aim of this study is to develop a preclinical model of blast-induced lower limb amputation.

Methods

Cadaveric Sprague-Dawley rats' left hindlimbs were exposed to blast waves of 7 to 13 bar burst pressures and 7.76 ms to 12.68 ms positive duration using a shock tube. Radiographs and dissection were used to identify the injuries.

Results

Higher burst pressures of 13 and 12 bar caused multiple fractures at the hip, and the right and left limbs. Lowering the pressure to 10 bar eliminated hip fractures; however, the remaining fractures were not isolated to the left limb. Further reducing the pressure to 9 bar resulted in the desired isolated fracture of the left tibia with a dramatic reduction in the fractures to other sites.

Conclusion

In this paper, a rodent blast injury model has been developed in the hindlimb of cadaveric rats that combines the blast and fracture in one insult, necessitating amputation. Experimental setup with 9 bar burst pressure and 9.13 ms positive duration created a fracture at the tibia with total reduction in non-targeted fractures, rendering 9 bar burst pressure suitable for translation to a survivable model to investigate blast injury-associated diseases.

Article focus

- This article focuses on developing a preclinical model of blast injury in the hindlimb of rats.
- It aims to achieve the blast-associated fracture and amputation in one insult, replicating the blast scenario.

Key messages

- The optimal experimental setup with 9 bar burst pressure and 9.13 ms positive duration produced the desired fracture at

the left hind tibia with total reduction in additional fractures.

Strengths and limitations

- The strength of this study is in achieving the blast-associated fracture in one insult using a shock tube without the need for an extra tool.
- The limitation of this study is in its cadaveric nature. Further translation of this model into a survivable model will allow the investigation of complications

Correspondence should be sent to Zepur Kazezian; email:
z.kazezian@ic.ac.uk

associated with blast injuries as well as high-energy road traffic accidents (RTAs).

Introduction

Blasts produced by improvised explosive devices (IEDs) are a major cause of injury in current and recent conflicts;[1,2] more than 70% of which are to the extremities,[3] of which half result in amputation.[4,5] This, combined with the dramatic increase in survivability of wounded service members from 70% in World War II to 88% in the Iraq wars,[6,7] has resulted in a large number of surviving amputees who face lifelong disability as a consequence of blast injuries. Blast-induced amputations are caused by combinations of primary blast, secondary blast due to fragments, and tertiary blast due to flail.[8-10] This study is concerned with amputations produced by primary and tertiary blasts as these are the most prevalent in conflicts.[9] These injuries can occur in the open air (OA), or in closed spaces (CS), such as within a vehicle; they are more prevalent in CS[4] and in the tibia.[11] Blast pressure in the OA scenario has a short positive phase duration, usually less than 10 ms, whereas the CS environment sustains the positive phase duration for much longer.[12]

Functional deficits due to blast-induced amputation include difficulty in weight-bearing and gait abnormalities.[13] Significant complications following traumatic amputations are pain in the residual limb[14] and phantom limb pain (PLP).[15] PLP is usually associated with biochemical changes in the brain and pathologies surrounding the amputated area including the skin, nerves, and vasculature.[16]

Another prevalent outcome of traumatic amputation due to blast is heterotopic ossification (HO).[17] This is the process of bone formation away from the skeleton within the surrounding soft tissues. This causes pain, swelling, and decreased range of motion and has a detrimental impact on quality of life.[18] HO can be hereditary or acquired. Blast-induced acquired HO in traumatic amputees has an incidence rate of approximately 64%.[19-22] To date, the mechanisms underlying HO development are not fully elucidated, resulting in non-specific therapeutic options such as non-steroidal anti-inflammatory drugs, radiation therapy, and, ultimately, surgery with a recurrence rate of 27%.[23-28]

Due to the ethical issues in accessing clinical results, and because limb salvage is the priority, studying the early stages of traumatic amputation-associated diseases such as HO in humans is challenging. This hinders the study of mechanisms associated with traumatic amputations. Hence, there is a need for in vivo models that fully replicate the combat scenario. Prior work has developed various rat models in which a shock tube is used to investigate the impact of different magnitudes and duration of the blast pressure in inducing inflammation.[29] Others used a pentaerythritol tetranitrate explosive, submerged beneath a water tank[30] or sand container[31] to induce the

Table I. Blast experimental design according to the different burst pressures.

Mean measured pressure, bar (SD)	Number of tests	Driver volume, %	Diaphragm thickness, μm	Mean positive phase duration, ms (SD)
12.97 (0.03)	6	100	300	12.68 (2.33)
12.03 (0.01)	8	100	200	12.16 (0.76)
10.01 (0.01)	7	100	150	9.69 (0.15)
9.01 (0.01)	8	100	150	9.13 (0.08)
7.00 (0.01)	5	100	100	7.76 (0.42)

SD, standard deviation.

fracture. The majority of these models used blast and a separate drop weight to create the fracture.[32-35]

Since the mechanisms that lead to PLP and HO formation after blast-induced traumatic amputation are not yet fully understood and need further investigation, and because studying HO in humans is difficult due to ethical issues, a survivable model of lower limb blast-induced amputation is required to enable the study of the mechanisms of blast injury. Existing in vivo HO models are limited in that bone fracture is not always achieved as a result of the blast itself, but by using an extra tool such as a drop weight to induce the bone fracture;[32-34] this does not replicate the exact scenario of combat-related blast injuries. Therefore, the aim of this study is to develop a blast injury model that combines the blast and the tibial fracture in one insult that results in a traumatic limb amputation. This study establishes the optimal experimental set-up and parameters in cadavers before using it in a survivable model.

Methods

Specimens. A total of 34 male Sprague-Dawley rat cadavers aged above 12 weeks and weighing 285 g to 481 g were used to optimize the burst pressure and positive phase duration period. All the procedures were approved and all personnel held personal licences from the Home Office to conduct these procedures.

Blast experimental set-up. The effect of primary and tertiary blast was modelled using a compressed air-powered shock tube that can replicate the blast loading conditions of various explosion scenarios. The driver section is pressurized with compressed air to the required firing pressure, which is regulated by a double breech system. As the burst pressure is reached, rupture of the diaphragms generates a blast wave that propagates along the driven section and subsequently reaches the cadaver at the end of the shock tube.[36] The platform used exposes only the left limb to the blast wave and protects other body parts, as prior work[29] has shown that even small blast pressures can elicit inflammatory responses in the rat.[37] Pressure sensors were mounted along the shock tube to monitor both the reproducibility of the blast wave produced (Sensor 1) and the output pressure close to the specimen (Sensor 2; Supplementary Figure a). Additionally, a
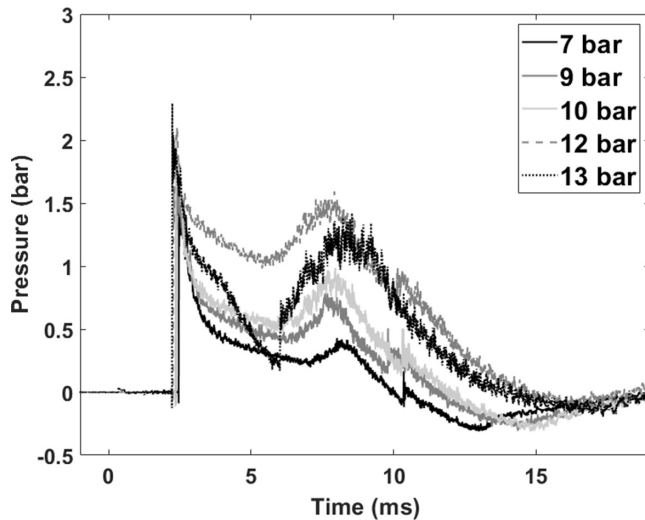
Fig. 1

Representative curves of different burst pressures measured by Sensor 2.

load-cell was mounted on the seat of the animal to measure the force on the rat's left hindlimb. Mylar diaphragms (DuPont, USA) of varying thicknesses were used to control the burst pressure and to control the magnitude of the shock wave produced (Table I). Since the positive phase duration of the shock wave is controlled by changing the volume of the driver section, we used 100% volume. This replicates a long positive phase duration blast scenario similar to that experienced in large-charge detonated devices in enclosed places such as inside a building or vehicle.

Experimental design of the blast injury model. In line with the 3Rs principle of replacement, reduction, and refinement, this study was conducted using cadaveric rats. Animals used were euthanized within 45 minutes prior to the experiments to avoid differences in body stiffness due to rigor mortis. All animals were subjected to a single blast with burst pressure of 7 to 13 bar, generated by the shock tube with 100% volume and 7.76 ms to 12.68 ms of positive phase duration. The aim was to expose the animal to primary and tertiary blast injury and achieve fracture of the left tibia. Each experiment was recorded by a Phantom camera version v210 (Vision Research, USA) with a high-powered lighting. The camera's frame rate was set at 28,000 frames/s. Video footage was analyzed using Phantom Camera Control Application Software (Vision Research). After the blast imposition, the specimens were x-rayed and dissected to identify and confirm the fractures.

Oscilloscope data collection and analysis. A digital oscilloscope was used to record at 50 MHz the data from each sensor fixed along the shock tube to monitor data reproducibility and to measure the actual pressure received by the left limb. The oscilloscope was triggered by the rising edge of the signal from Sensor 1. Data were analyzed using MATLAB (version R2020a; MathWorks, USA).

Radiograph collection and analysis. A Fluoroscan InSight FD Mini C-Arm system (Hologic, USA) was used to image the rat limbs (imaging parameters: 49 kV, 0.056 mA). ImageJ V1.52q (National Health Institute, USA) was used to analyze the radiographs.[38]

Statistical analysis. All data are presented as mean and standard deviation (SD). One-way repeated measures analysis of variance (ANOVA) was applied with Tukey-Kramer post-hoc test to assess the significance of each blast parameter (peak pressure, impulse, and positive phase duration) and the force at different pressures with a statistical significance level set at $p < 0.05$ using GraphPad Prism 8 (version 8.4.2; GraphPad Software, USA).

Results

The characteristics of the blast waves of different burst pressures. All blast waves generated demonstrated a classic pattern including a positive incident pressure which is followed by a negative under-pressure and consequent gain back of the ambient pressure (Figure 1). Loading parameters are presented in Figure 2. Peak pressure reduced significantly ($p < 0.001$, one-way ANOVA) with burst pressure reduction from 13 bar (mean 2.25 bar (SD 0.11)) to 12 bar (mean 2.11 bar (SD 0.09)), 10 bar (mean 2.02 bar (SD 0.03)), 9 bar (mean 1.95 bar (SD 0.02)), and 7 bar (mean 1.69 bar (SD 0.05)) (Figure 2a). Similarly, positive phase duration (Figure 2b) significantly reduced from 13 bar (mean 12.68 ms (SD 2.33)) to 10 bar (mean 9.69 ms (SD 0.15)), 9 bar (mean 9.13 ms (SD 0.08)), and 7 bar (mean 7.76 ms (SD 0.42)). In parallel, significantly shorter positive phase duration was noted in 10 bar, 9 bar, and 7 bar compared to 12 bar. Surprisingly, impulse (Figure 2c) did not reduce from 13 (mean 9.30 bar ms (SD 2.45)) to 12 bar (mean 10.30 bar ms (SD 1.61)); however, impulse decreased with burst pressure reduction from 12 to 10 bar (mean 5.83 bar ms (SD 0.18)), 9 bar (mean 4.59 bar ms (SD 0.08)), and 7 bar (mean 2.86 bar ms (SD 0.05)). Although forces measured on the left limb decreased as the burst pressure was reduced, these changes were not significant and were: 13 bar (mean 132.84 N (SD 14.28)), 12 bar (mean 124.60 N (SD 22.78)), 10 bar (mean 118.93 N (SD 35.85)), 9 bar (mean 107.63 N (SD 16.98)), and 7 bar (mean 100.38 N (SD 16.99)).

High magnitudes of burst pressures resulted in several fractures in the hip and both limbs of the rats. Left tibia fractures were the desired outcome. The radiological analysis compared to the control (Intact rat, no injuries) (Figure 3a) found that, in addition to the desired outcome, for 13 bar pressure (Figure 3b) most rats had hip fractures (5/6) and for 12 (Figure 3c) and 13 bar pressures all rats had right limb above- and below-knee fractures and left limb above-knee fractures (Table II). A reduction of the burst pressure to 10 bar (Figure 3d) reduced the above-knee fractures in the right limb to 2/7 rats but did not reduce the above-knee fractures in the left limb (Table II). The optimal burst pressure of 9 bar (Figure 3e) resulted in no hip fractures, 2/8 right limb fractures, 3/8 above-knee
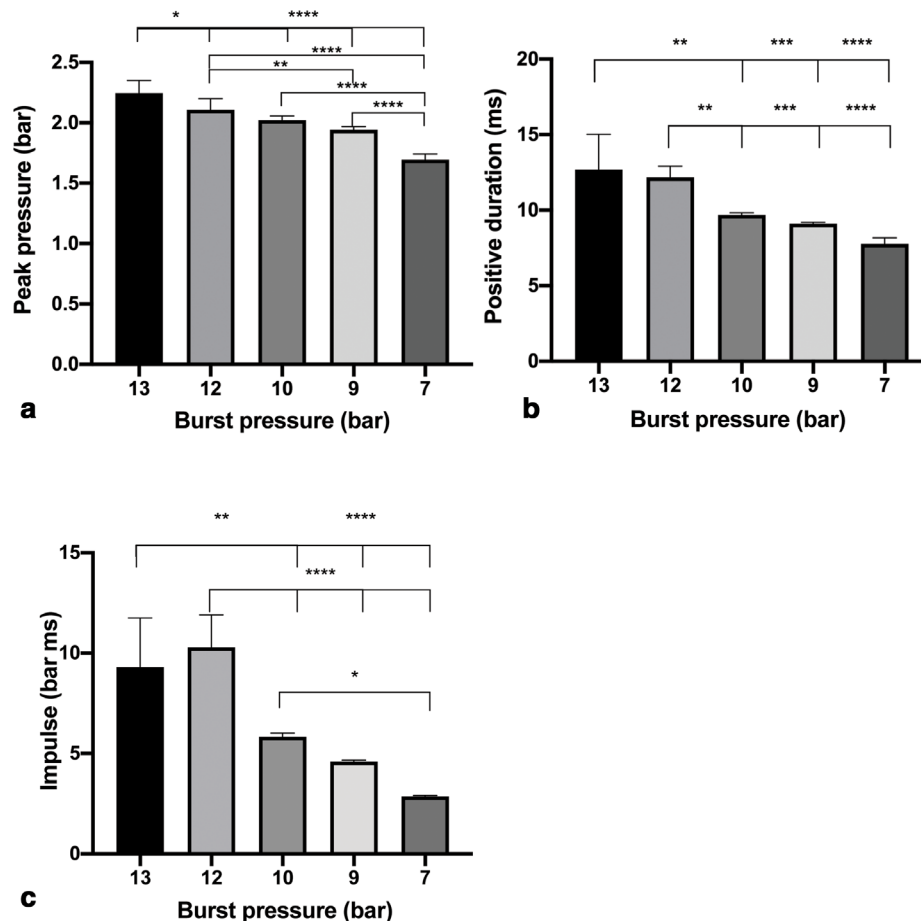
Fig. 2

Blast loading parameters: a) peak pressure; b) positive phase duration; and c) impulse. Data are presented as mean and standard deviation (SD). *p < 0.05, **p < 0.01, ***p < 0.001, ****p < 0.0001.

fractures in the left limb, and 8/8 desired below-knee fractures in the left limb (Supplementary Video 1). Reduction of the burst pressure to 7 bar (Figure 3f) resulted in no fractures.

The video footage was scrutinized to investigate the cause of the undesired additional fractures. This identified that, at 9 and 10 bar pressures, the animals of small size (285 g to 293 g) moved within the platform to enable both of the limbs to hit the platform outlets, thus causing the undesired knee fractures. Similarly, large animals (450 g to 481 g) did not fit comfortably in the designed seat of the platform that also resulted in fractures in the non-targeted sites. The medium-sized animals (320 g to 430 g) had no undesired fractures.

Discussion
The aim of this study was to develop an in vivo survivable primary and tertiary blast injury model to replicate the injuries seen due to an IED detonation scenario in enclosed spaces. Specifically, this required that, in one blast insult, an isolated tibial fracture should be induced that would subsequently require amputation. This pilot cadaveric work established the shock tube experimental configuration, including defining the acceptable size of rats and optimal burst pressure requirements. An upper pressure threshold was found above which multiple non-desired fractures occurred to the hips and contralateral limbs; this would be unlikely to translate to a survivable model. A lower threshold was found below which no fractures occurred. The 9 bar pressure resulted in the desired left tibia fracture as well as some additional lower limb fractures. The cause of the additional fractures was that some animals were too small and so were more prone to multiple fractures at the location of the growth plates. The age of sexual maturity of rats varies between subjects from postnatal (P) 40 days to P 76 days in males.[39] Weight is an indicator of skeletal maturity; Sprague-Dawley rats that weigh 300 g are defined as young adolescents.[40] Around 25% of the animals in the 9 bar group were in this adolescent range, which partly explains the unnecessary fractures. Additionally, rats above 450 g did not fit comfortably in the designed seat of the platform and these also had additional undesired fractures. Therefore, based on our experience with the rat weights and experimental apparatus, this pilot study recommends that only animals weighing between 320 g and 430 g are used
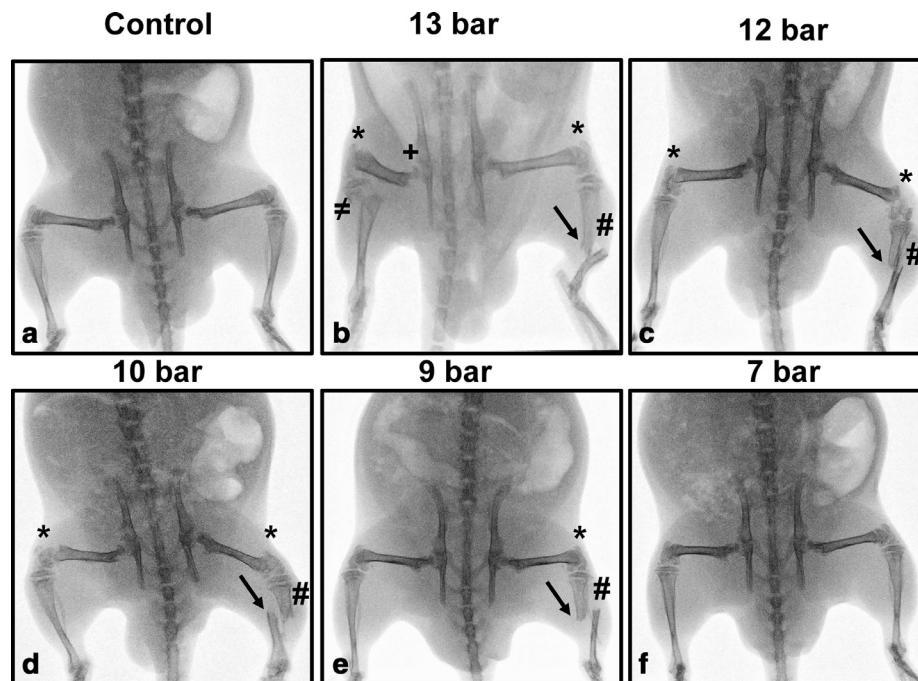
Fig. 3

Representative radiographs at each level of burst pressures. Dorsal capture of: a) control (intact rat); b) 13 bar; c) 12 bar; d) 10 bar; e) 9 bar; and f) 7 bar burst pressure. Fractures are annotated as follows: +hip fracture; ≠below-knee fracture; *above knee fracture; and #tibial fracture at the intended site (left hindlimb), also indicated by arrows.

Table II. The different fractures identified as a result of each burst pressure on the hip, right limb, and left limb.

Burst pressure, bar	Rats, n	Hip fractures, n	Right limb fractures, n	Left limb fractures, n	Aimed left limb tibial fractures, n	Body mass, g
13	6	5	6	6	6	306 to 430
12	8	0	8	8	8	307 to 430
10	7	0	5	7	7	290 to 375
9	8	0	2	3	8	285 to 481
7	5	0	0	0	0	348 to 419

as outside this range, there is the chance of above- and below knee fractures at 9 bar.

IED detonations are estimated to generate blast waves of 50 kPa to 1,000 kPa peak pressure with a positive duration of 2 ms to 6 ms.[41] The blast pressure in this study (900 kPa) is close to the top of this range, however, the pressure registered by Sensor 2 – i.e. reached the animal – is 195 kPa. This is slightly higher than the pressure used in previous in vivo experiments (120 Pa (SD 7)), which aimed to establish similar models in rats.[32-35] The higher pressure in our study would explain why, in our model, the fracture was achieved while the other models did not achieve the desired fracture in a single blast exposure, but induced the fracture through an extra drop weight.

This cadaveric model will now be translated into a survivable model to investigate the early mechanisms of blast injury-associated diseases monitored over several timepoints. In a further application, this model may also be used to study amputation from RTA, as the duration of road traffic collisions are between 10 ms and 20 ms,[42] similar to the positive duration of the blast wave used in our model. Also, the impact loading on the limb during RTA also has a near instantaneous rise, similar to that in blast. In fact, other blast experiments use impacting materials to produce blast loading rates.[43,44]

In summary, to our knowledge, this article presents the first blast injury model that combines the blast and blast-associated injury to the lower limb without the use of an extra insult to induce the fracture, thus replicating the scenario of IED detonation in enclosed vehicles. Our findings show that 9 bar burst pressure for rats weighing between 320 g and 430 g can achieve a single fracture of the tibia. This model is now being translated into a survivable blast-associated traumatic amputation model to study mechanisms of blast injury conditions such as HO. This model also could be used to study other trauma amputations such as those due to high-energy RTAs.

Twitter

Follow Z. Kazezian @DKazezian
Follow A. M. J. Bull @Biomechanics14

Supplementary material

ë A diagram of the shock tube and blast platform, and a representative video of the cadaveric blast injury model at 9 bar.

References

1. **Ramasamy A**, **Harrisson SE**, **Stewart MPM**, **Midwinter M**. Penetrating missile injuries during the Iraqi insurgency. *Ann R Coll Surg Engl*. 2009;91(7):551–558.
2. **Beckett A**, **Pelletier P**, **Mamczak C**, **Benfield R**, **Elster E**. Multidisciplinary trauma team care in Kandahar, Afghanistan: current injury patterns and care practices. *Injury*. 2012;43(12):2072–2077.
3. **Ramasamy A**, **Harrisson SE**, **Clasper JC**, **Stewart MPM**. Injuries from roadside improvised explosive devices. *J Trauma*. 2008;65(4):910–914.
4. **Ramasamy A**, **Masouros SD**, **Newell N**, **et al**. In-vehicle extremity injuries from improvised explosive devices: current and future foci. *Philos Trans R Soc Lond B Biol Sci*. 2011;366(1562):160–170.
5. **Smith S**, **Devine M**, **Taddeo J**, **McAlister VC**. Injury profile suffered by targets of antipersonnel improvised explosive devices: prospective cohort study. *BMJ Open*. 2017;7(7):e014697.
6. **Hofmeister EP**, **Mazurek M**, **Ingari J**. Injuries sustained to the upper extremity due to modern warfare and the evolution of care. *J Hand Surg Am*. 2007;32(8):1141–1147.
7. **Mazurek MT**, **Ficke JR**. The scope of wounds encountered in casualties from the global war on terrorism: from the battlefield to the tertiary treatment facility. *J Am Acad Orthop Surg*. 2006;14(Supplement):S18–S23.
8. **Ramasamy A**, **Hill AM**, **Masouros S**, **Gibb I**, **Bull AMJ**, **Clasper JC**. Blast-Related fracture patterns: a forensic biomechanical approach. *J R Soc Interface*. 2011;8(58):689–698.
9. **Singleton JAG**, **Gibb IE**, **Bull AMJ**, **Clasper JC**. Blast-mediated traumatic amputation: evidence for a revised, multiple injury mechanism theory. *J R Army Med Corps*. 2014;160(2):175–179.
10. **Trimble K**, **Clasper J**. Anti-personnel mine injury; mechanism and medical management. *J R Army Med Corps*. 2001;147(1):73–79.
11. **Hull JB**, **Bowyer GW**, **Cooper GJ**, **Crane J**. Pattern of injury in those dying from traumatic amputation caused by bomb blast. *Br J Surg*. 1994;81(8):1132–1135.
12. **Chaloner E**. Blast injury in enclosed spaces. *BMJ*. 2005;331(7509):119–120.
13. **Farrokhi S**, **Mazzone B**, **Moore JL**, **Shannon K**, **Eskridge S**. Physical therapy practice patterns for military service members with lower limb loss. *Mil Med*. 2019;184(11-12):e907–e913.
14. **Neil MJE**. Pain after amputation. *BJA Education*. 2016;16(3):107–112.
15. **Richardson C**, **Kulkarni J**. A review of the management of phantom limb pain: challenges and solutions. *J Pain Res*. 2017;10:1861–1870.
16. **Guo X**, **Lyu Y**, **Wang Z**, **et al**. Correlates of residual limb pain: from residual limb length and usage to metabolites and activity in secondary somatosensory cortex. *IEEE Trans Neural Syst Rehabil Eng*. 2019;27(1):96–104.
17. **Puzas JE**, **Miller MD**, **Rosier RN**. Pathologic bone formation. *Clin Orthop Relat Res*. 1989;245:269–81.
18. **Dey D**, **Wheatley BM**, **Cholok D**, **et al**. The traumatic bone: trauma-induced heterotopic ossification. *Transl Res*. 2017;186:95–111.
19. **Alfieri KA**, **Forsberg JA**, **Potter BK**. Blast injuries and heterotopic ossification. *Bone Joint Res*. 2012;1(8):174–179.
20. **Brown KV**, **Dharm-Datta S**, **Potter BK**, **et al**. Comparison of development of heterotopic ossification in injured US and UK armed services personnel with combat-related amputations: preliminary findings and hypotheses regarding causality. *J Trauma*. 2010;69 Suppl 1:–S116–S122.
21. **Potter BK**, **Burns TC**, **Lacap AP**, **Granville RR**, **Gajewski D**. Heterotopic ossification in the residual limbs of traumatic and combat-related amputees. *J Am Acad Orthop Surg*. 2006;14(10 Spec No.):S191–S197.
22. **Forsberg JA**, **Pepek JM**, **Wagner S**, **et al**. Heterotopic ossification in high-energy wartime extremity injuries: prevalence and risk factors. *J Bone Joint Surg Am*. 2009;91-A(5):1084–1091.
23. **Barfield WR**, **Holmes RE**, **Hartsock LA**. Heterotopic ossification in trauma. *Orthop Clin North Am*. 2017;48(1):35–46.
24. **Nauth A**, **Giles E**, **Potter BK**, **et al**. Heterotopic ossification in orthopaedic trauma. *J Orthop Trauma*. 2012;26(12):684–688.
25. **Edwards DS**, **Clasper JC**. Heterotopic ossification: a systematic review. *J R Army Med Corps*. 2015;161(4):315–321.
26. **Shehab D**, **Elgazzar AH**, **Collier BD**. Heterotopic ossification. *J Nucl Med*. 2002;43(3):346–353.
27. **Teasell RW**, **Mehta S**, **Aubut JL**, **et al**. A systematic review of the therapeutic interventions for heterotopic ossification after spinal cord injury. *Spinal Cord*. 2010;48(7):512–521.
28. **Pavey GJ**, **Polfer EM**, **Nappo KE**, **Tintle SM**, **Forsberg JA**, **Potter BK**. What risk factors predict recurrence of heterotopic ossification after excision in combat-related amputations? *Clin Orthop Relat Res*. 2015;473(9):2814–2824.
29. **Eftaxiopoulou T**, **Barnett-Vanes A**, **Arora H**, **et al**. Prolonged but not short-duration blast waves elicit acute inflammation in a rodent model of primary blast limb trauma. *Injury*. 2016;47(3):625–632.
30. **Tannous O**, **Griffith C**, **O'Toole RV**, **Pellegrini VD**. Heterotopic ossification after extremity blast amputation in a Sprague-Dawley rat animal model. *J Orthop Trauma*. 2011;25(8):506–510.
31. **Jaffe DE**, **Yoo D**, **Blevins J**, **et al**. Does blast medium affect heterotopic ossification in a Blast-amputation model? *Clin Orthop Relat Res*. 2015;473(8):2680–2687.
32. **Qureshi AT**, **Crump EK**, **Pavey GJ**, **Hope DN**, **Forsberg JA**, **Davis TA**. Early characterization of blast-related heterotopic ossification in a rat model. *Clin Orthop Relat Res*. 2015;473(9):2831–2839.
33. **Pavey GJ**, **Qureshi AT**, **Hope DN**, **et al**. Bioburden increases heterotopic ossification formation in an established rat model. *Clin Orthop Relat Res*. 2015;473(9):2840–2847.
34. **Polfer EM**, **Hope DN**, **Elster EA**, **et al**. The development of a rat model to investigate the formation of blast-related post-traumatic heterotopic ossification. *Bone Joint J*. 2015;97-B(4):572–576.
35. **Qin MY**, **Atwood RE**, **Ketchum WA**, **Kaba SA**, **Bradley MJ**. Characterization of serum levels of testosterone and corticosterone in a blast and amputation rat model of heterotopic ossification. *Mol Cell Endocrinol*. 2020;509:110799.
36. **Nguyen T-T**, **Pearce AP**, **Carpanen D**, **et al**. Experimental platforms to study blast injury. *J R Army Med Corps*. 2019;165(1):33–37.
37. **Barnett-Vanes A**, **Sharrock A**, **Eftaxiopoulou T**, **et al**. CD43Lo classical monocytes participate in the cellular immune response to isolated primary blast lung injury. *J Trauma Acute Care Surg*. 2016;81(3):500–511.
38. **Brookes SJ**, **ImageJ U**. Using ImageJ (Fiji) to analyze and present X-ray CT images of enamel. *Methods Mol Biol*. 2019;1922:267–291.
39. **Lewis EM**, **Barnett JF**, **Freshwater L**, **Hoberman AM**, **Christian MS**. Sexual maturation data for CRL Sprague-Dawley rats: criteria and confounding factors. *Drug Chem Toxicol*. 2002;25(4):437–458.
40. **McCutcheon JE**, **Marinelli M**. Age matters. *Eur J Neurosci*. 2009;29(5):997–1014.
41. **Panzer MB**, **Wood GW**, **Bass CR**. Scaling in neurotrauma: how do we apply animal experiments to people? *Exp Neurol*. 2014;261:120–126.
42. **Ghajari M**, **Hellyer PJ**, **Sharp DJ**. Computational modelling of traumatic brain injury predicts the location of chronic traumatic encephalopathy pathology. *Brain*. 2017;140(2):333–343.
43. **Radford DD**, **Deshpande VS**, **Fleck NA**. The use of metal foam projectiles to simulate shock loading on a structure. *Int J Impact Eng*. 2005;31(9):1152–1171.
44. **Bustamante MC**, **Singh D**, **Cronin DS**. Polymeric Hopkinson bar-confinement chamber apparatus to evaluate fluid cavitation. *Exp Mech*. 2018;58(1):55–74.

Author information:
- Z. Kazezian, PhD, Post-doctoral Research Associate
- M. Ramette, MSc, PhD Student
- A. M. J. Bull, PhD, FREng, Professor of Musculoskeletal Mechanics
  Centre for Blast Injury Studies, Imperial College London, London, UK; Department of Bioengineering, Imperial College London, London, UK.
- X. Yu, MEng, PhD Student, Centre for Blast Injury Studies, Imperial College London, London, UK; Dyson School of Design Engineering, Imperial College London, London, UK.
- W. Macdonald, PhD, Senior Teaching Fellow, Department of Bioengineering, Imperial College London, London, UK.